

High-precision Eddy-current Tip Clearance Sensor with Exceptional Heat Resistance

Fu-lin Liu[1], Ling-qiang Zhao[1], Ya-guo Lyu[1], Bo-sen Chang[1], Zhen-xia Liu[1],
[1]School of Power and Energy, Northwestern Polytechnical University, Xi'an 710129, China

Abstract

Eddy current sensors are increasingly being used to measure dynamic tip clearances in turbines due to their excellent resistance to interference and the advantages of non-contact measurement. However, the core component of an eddy current sensor is the probe's sensing coil, whose output characteristics are highly sensitive to temperature changes. The high temperatures and wide temperature fluctuations inside the engine directly affect the sensor's output characteristics, leading to significant errors in gap measurement. Therefore, conducting in-depth research into the impact of temperature on the performance of eddy current sensors and developing effective temperature compensation strategies are of great significance for the accurate measurement of blade tip gaps. To this end, this paper describes the fabrication of a high-temperature-resistant eddy current sensor using platinum wire as the material; subsequently, using a combination of numerical simulation and experimental testing, the measurement performance of the fabricated sensor was systematically evaluated, with a particular focus on its output stability and accuracy under high-temperature conditions; based on the results of the experimental study, a measurement scheme for an eddy current tip clearance sensor suitable for high-temperature environments was ultimately proposed, and a prototype was successfully developed.

The main conclusions of this paper are as follows: experimental data indicate that temperature causes changes in the equivalent inductance and equivalent resistance of the eddy current sensor; furthermore, at different clearances, the effect of temperature on the equivalent inductance of the eddy current sensor is significantly greater than its effect on the equivalent resistance, which is the primary cause of temperature drift errors in eddy current sensors. Based on this characteristic, the paper designs an eddy current sensor measurement circuit based on analytical inductance. Experimental data show that the designed eddy current sensor exhibits reduced temperature sensitivity, as well as a wide measurement range and high measurement accuracy.

Keywords: Aero-engine; Eddy current sensor; Blade tip clearance; Temperature compensation; High precision.

https://doi.org/10.71945ICAS2026_0483

1. Introduction

Aviation engines operate continuously under harsh conditions characterised by high speeds, high temperatures and heavy loads. As the core working components of the engine, the operating conditions of the turbine and compressor directly affect the overall performance of the aviation engine [1]. In gas turbine engines, there is a gap between the tips of the rotor blades of the compressor and turbine and the outer casing, known as the tip clearance [2]. Generally, the tip clearance is only 1% to 3% of the blade height; however, this clearance can vary significantly when the engine operating conditions change [3]. The magnitude of the radial tip clearance in aeroengine rotor blades has a significant impact on engine performance (primarily including surge margin, specific fuel consumption (SFC) and compressor efficiency) [4-6]. Reducing the radial tip clearance of the compressor rotor blades can improve engine performance; however, excessively small clearances may also increase the risk of tip-to-casing contact and wear [7-9]. Therefore, it is essential to design and control the rotor tip clearance appropriately. Closed-loop active tip clearance control represents the future direction of active tip clearance control, and it relies on reliable online measurement technology for tip clearance.

Over the past few decades, a variety of gap measurement sensors based on different measurement principles have been developed and put into use, including optical, capacitive, microwave and eddy current methods. Among these, fibre-optic sensors offer high-precision measurement capabilities; such probes are compact in size and are not restricted by blade structure or material, but their surfaces are susceptible to contamination from soot, oil and dust [10][11]. Capacitive sensors are widely used in gap measurement due to their simple structure and low cost; however, their output results are subject to interference from factors such as the humidity and pressure of the gas between the capacitor plates, which limits the application of this type of sensor in measuring the tip-to-tip gaps of aeroengine turbine blades[12]. Although microwave sensors possess characteristics such as high-temperature resistance and resistance to gas corrosion, the spatial filtering effect limits their application within aeroengines[13]. In contrast, eddy current sensors have attracted widespread attention in the field of aeroengine rotor blade tip gap measurement due to their advantages of strong anti-interference capability, fast response speed, high sensitivity, non-contact measurement, and immunity to medium contamination [14-17].

In practical tip clearance measurements, the temperature of the measurement environment can reach as high as 1000 °C, and this temperature fluctuates dramatically depending on the operating conditions of the aeroengine [18]. As the physical properties of the internal metal coils in eddy current sensors are highly susceptible to temperature changes, such drastic temperature fluctuations directly affect the sensor's performance, thereby compromising the accuracy of the clearance measurements.

Current research on eddy current sensors has primarily focused on the effects on sensor output characteristics in environments below 500°C. Although some researchers have demonstrated and experimentally verified the feasibility of using eddy current sensors to measure blade tip clearances in aeroengines, they have not considered the impact of temperature on the accuracy of measurement results; moreover, research into the output characteristics of eddy current sensors under high-temperature environments and over a wide range of temperature variations remains limited. The most established temperature compensation method at present involves installing additional temperature probes to measure the internal temperature of the aeroengine simultaneously; however, this method requires drilling additional holes in the inner wall of the engine casing, which affects the engine's aerodynamic performance. Furthermore, localised high temperatures may cause the temperature probes to fail, thereby increasing measurement errors in the gap measurement.

It is therefore particularly important to conduct in-depth research into the effect of temperature on the performance of eddy current sensors and to implement effective compensation measures, in order to ensure that reliable measurement results can still be obtained in extreme environments. Starting from the detection principles of eddy current sensors, this paper describes the fabrication of an eddy current sensor probe suitable for measuring blade tip clearances in aeroengines. Tests

were conducted on its measurement performance and adaptability to high-temperature environments, revealing the mechanism by which temperature causes measurement errors in eddy current sensors, and proposing a signal analysis method for eddy current sensors suitable for high-temperature environments. This research will help enhance the gap measurement capability and reliability of sensors in high-temperature environments, laying a theoretical and practical foundation for the development of intelligent maintenance and condition monitoring technologies for aeroengines.

2. Working principle

2.1 The principle of operation

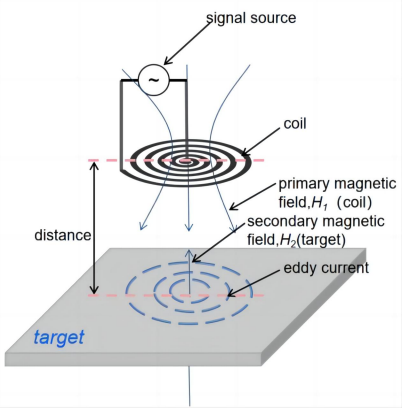


Figure 1 -Schematic diagram of the eddy current sensor measurement principle

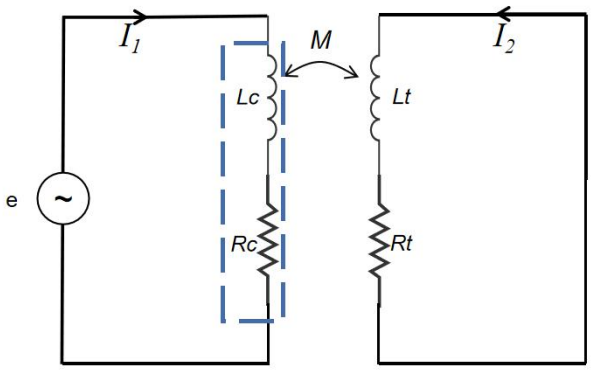


Figure 2 -Equivalent circuit model of an eddy current sensor

The basic principle of eddy current gap measurement is illustrated in Figure 1. According to Maxwell's and Ampère's laws, when an alternating current signal is applied to the eddy current sensor, a varying magnetic field (i.e. the primary magnetic field H_1) is generated at the front of the sensor probe. When the sensor probe approaches a metallic target, the varying magnetic field induces loop currents (also known as eddy currents) within and on the surface of the metallic target; simultaneously, these loop currents generate a secondary magnetic field H_2 on the surface of the target. According to Lenz's Law, the direction of the secondary magnetic field is opposite to that of the primary magnetic field; the secondary magnetic field acts to reduce the primary magnetic field, causing changes in the amplitude and phase of the current within the probe coil. This change is captured by the sensor, thereby enabling gap measurement. This process can be represented as a closed-loop model, as shown in Figure 2. In this model, the inductance and resistance of the eddy current sensor coil are denoted by L_C and R_C, whilst the inductance and resistance of the target are denoted by L_t and R_t. I_1 represents the high-frequency current applied to the coil by the excitation source, and I_2 represents the eddy currents generated by the target.

According to Kirchhoff's law

$$\begin{cases} (R_c + \mathrm{j}wL_c)I_1 - jwMI_2 = \tilde{e} \\ -jwMI_1 + (R_t + jwL_t)I_2 = 0 \end{cases} \tag{1}$$

In the equation, M represents the mutual inductance between the sensor coil and the conductor under test, and is given by $M=k\sqrt{L_cL_t}$ (where k is the coupling coefficient between the two, which depends on three main factors: the coil structure, their relative positions, and the characteristics of the magnetic medium; $0 < k < 1$). Solving this system of equations yields I_1 as

$$I_1 = \frac{e}{R_c + \dfrac{w^2M^2}{R_t^2 + (wL_t)^2}R_t + j\left[wL_c - \dfrac{w^2M^2}{R_t^2 + (wL_t)^2}wL_t\right]} \tag{2}$$

Therefore, the equivalent impedance Z of the coil is

$$Z = \frac{e}{I_1} = R_c + \frac{w^2 M^2}{R_t^2 + (wL_t)^2} R_t + j\left[wL_c - \frac{w^2 M^2}{R_t^2 + (wL_t)^2} wL_t \right] \tag{3}$$

That is, the equivalent inductance and equivalent resistance of the coil are

$$\begin{cases} R = R_c + \dfrac{w^2 M^2}{R_t^2 + (wL_t)^2} R_t \\ L = L_c - \dfrac{w^2 M^2}{R_t^2 + (wL_t)^2} L_t \end{cases} \tag{4}$$

In Equations (3) and (4), R and L denote the equivalent resistance and equivalent inductance of the coil, whilst R_C and L_C denote the DC resistance and DC inductance of the coil.

Based on the above principle, as shown in Equation 5, the output impedance Z of the eddy current sensor is a function of the excitation signal, the coil impedance parameters, and the physical properties of the target object.

$$Z = f(L, R, d, \mu_1, \sigma_1, \mu_2, \sigma_2, f_c) \tag{5}$$

Here, L represents the inductance of the coil, R represents the resistance of the coil, μ_1 and σ_1 represent the magnetic permeability and electrical conductivity of the coil material respectively, μ_2 and σ_2 represent the magnetic permeability and electrical conductivity of the target object respectively, and f represents the excitation frequency of the excitation source.

As can be seen from Equations 3 and 5, when the air gap changes, the impedance Z, quality factor Q and inductance L of the eddy current sensor all change. In theory, any one of these three parameters may be selected and converted into a voltage or current to serve as the sensor's output parameter. The sensor's sensitivity and the magnitude of the output value are related to the parameters of the excitation signal, the structure of the sensor coil, and the electrical and magnetic permeability of the target object; however, when the sensor specifications, excitation signal parameters and target material are all fixed, the sensor's output impedance can be expressed as a single-valued function of the gap value, namely

$$Z = f(d) \tag{6}$$

Changes in the coil impedance cause a shift in the voltage division ratio of the measurement circuit, thereby enabling the detection of gap parameters. However, when the ambient temperature fluctuates, the equivalent R_C resistance of the sensor changes, which in turn alters the coil impedance and ultimately introduces measurement errors.

3. Method

3.1 Numerical Simulation Research

3.1.1 Numerical simulation model

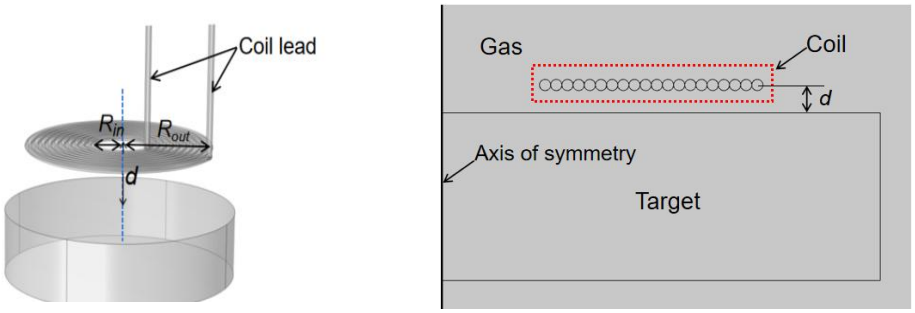
This paper employs the finite element analysis method to investigate the output characteristics of the sensor. Based on the measurement principle of eddy current sensors, a numerical simulation model, as shown in Figure 3, was constructed in the finite element simulation software COMSOL. The simulation parameters are shown in Table 1. In Figures 3(a), R_{in} represents the inner diameter of the coil, R_{out} represents the outer diameter of the coil, and d represents the gap between the coil and the target object. The annular coil is made of platinum, and the target object is a nickel-based alloy rod with a diameter of 20mm and a height of 5mm. The material parameters within the computational domain are shown in Table 2; the remaining volume consists of air at standard atmospheric conditions at 20°C.

Table 1 Simulation parameters

Parameters	Value	Unit	Description
N	20	1	Number of coil turns
H	1	1	Number of coil layers
Dwire	0.2	mm	Coil wire diameter
f	1	MHz	Stimulation frequency
U	2	Vpp	Excitation voltage
d	0~4	mm	Gap range
T	20~500	℃	Temperature range

Table 2: Coil Material Parameters

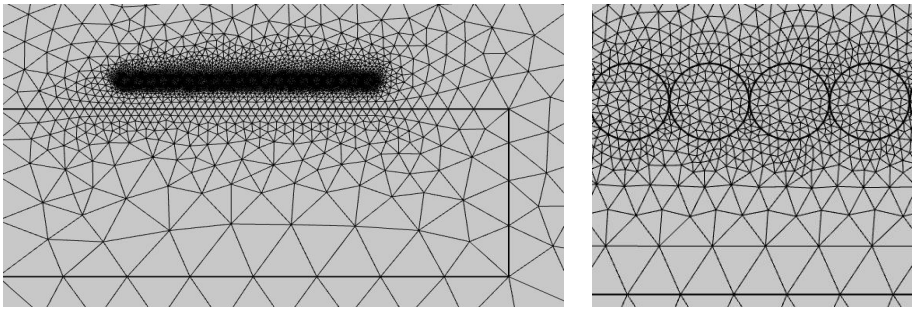
Name	melting point/℃	Electrical conductivity/MS·m-1	Temperature coefficient of resistance/10-6·℃	Coefficient of thermal expansion/10-6·k-1	Relative magnetic permeability
Pt	1768	6.7	3920	8.8	1
Inconel625	1455	1.01	4.791	12.8	1



(a)Schematic diagram of a 3D model (b)Two-dimensional axisymmetric model

Figure 3 -Simulation model

The mesh was automatically generated using COMSOL. A triangular mesh was employed for the computational domain, with mesh refinement applied around the coil. The total number of mesh elements is 7,985, and the average mesh quality is 0.95.



(a) Overall grid division (b) Coil-reinforced mesh

Figure 4 -Finite element simulation meshing

3.1.2 Simulation results

Using the AC/DC Module and the Circuit Interface in COMSOL software, a voltage divider circuit for an eddy current sensor was constructed, as shown in Figure 5. The excitation signal is 3Vpp at 1 MHz, and the value of the series resistor R_1 is 7.5 Ω. When the ambient temperature varies, the curve showing the sensor output voltage as a function of the air gap is shown in Figure 6.

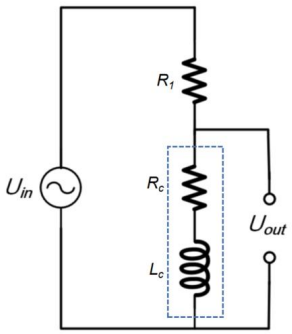


Figure 5 -Schematic diagram of a voltage divider circuit

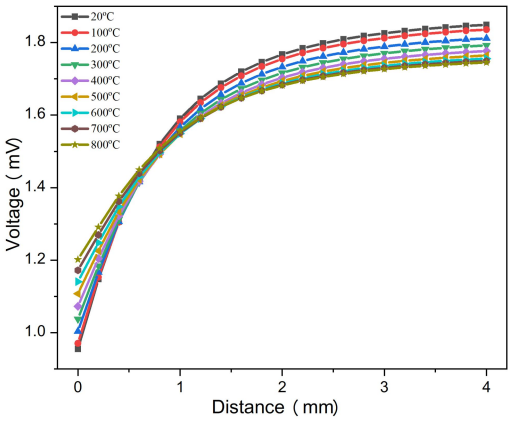


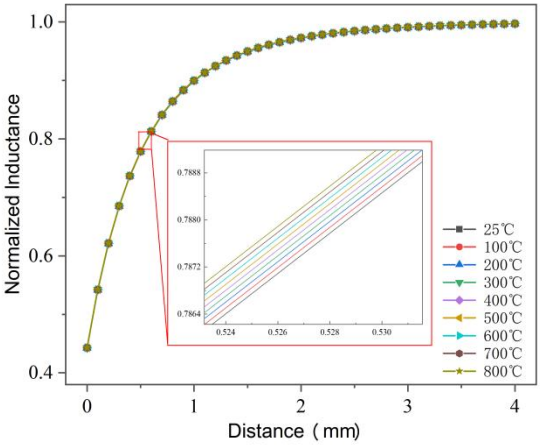
Figure 6 -Numerical simulation of voltage variation curves

The simulation results indicate that, when the measured gap remains constant, temperature variations cause a significant deviation in the sensor's output voltage; moreover, the higher the temperature, the greater the difference between the output voltage and that under standard temperature conditions. This pattern is consistent with the theoretical conclusions derived from Equation (4), suggesting that eddy current sensors calibrated at standard temperature are not suitable for high-temperature conditions; when the ambient temperature fluctuates significantly, the sensor's output signal will become distorted.

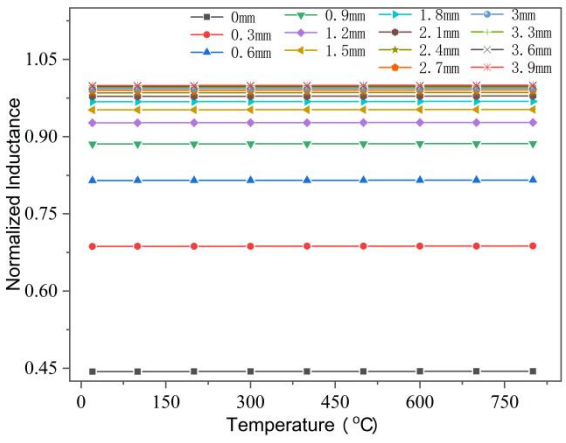
To analyse the mechanism underlying this error in greater depth, Figures 7 and 8 illustrate the variation in the sensor coil's resistance and inductance under different air gap and temperature conditions. To simplify the analysis, the coil inductance data has been normalised; the specific calculation method is shown in Equation (7).

$$\overline{L} = \frac{L_i}{L_{\max}} \tag{7}$$

Here, $\overline{L}$ represents the normalised inductance value, L_i represents the inductance value under different operating conditions, and $L_{\max}$ represents the maximum inductance value across all operating conditions.

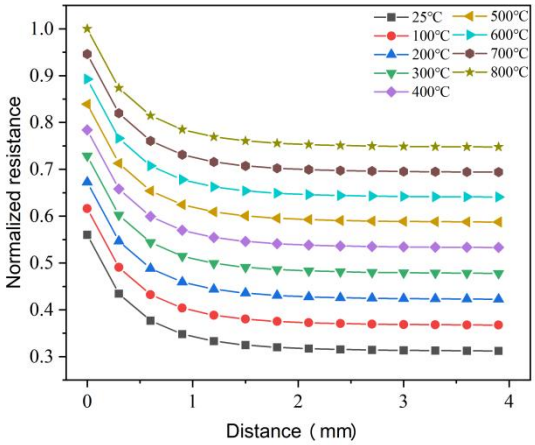


(a)Variation in the equivalent inductance of an eddy current sensor with displacement at different temperatures

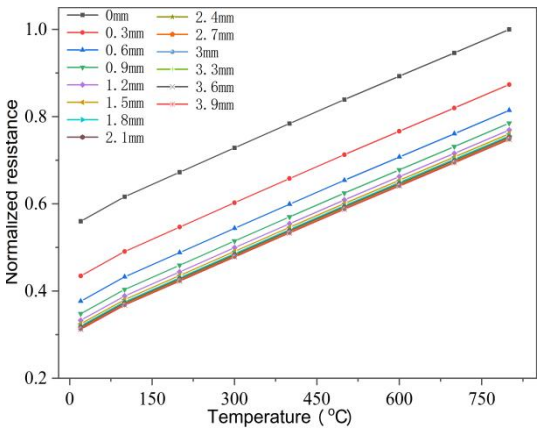


(b)Temperature-dependent variation in the equivalent inductance of an eddy current sensor at different air gaps

Figure 7 -Variation curve of the equivalent inductance of an eddy current sensor



(a)Variation in the equivalent resistance of an eddy current sensor with displacement at different temperatures



(b)Temperature-dependent equivalent resistance of eddy current sensors at different gaps

Figure 8 -Variation curve of the equivalent resistance of an eddy current sensor

Analysis of the results in Figure 7 shows that the normalised inductance of the coil increases as the measured gap widens, whilst the inductance sensitivity gradually decreases with increasing gap. When the gap *d* exceeds 2.5 mm, the inductance sensitivity drops to an extremely low level; within the measurement range of 2.5~4 mm, the overall variation in inductance accounts for only 2.59% of the full scale. This characteristic results in a significant reduction in measurement resolution and accuracy when the eddy current sensor is used to measure large gaps. Compared to the gap, the influence of temperature on the inductance parameters is very limited: under the same gap conditions, when the ambient temperature rises from room temperature to 800 °C, the change in inductance is less than 0.181% of the room-temperature reference value.

Figure 8 shows the characteristic curve of the sensor's equivalent resistance as a function of gap and temperature. The data indicate that the normalised resistance decreases gradually as the gap increases, with a steeper rate of decline in the small gap range; as the gap increases further, the change in equivalent resistance tends to level off. Within the 0~2 mm measurement range, the maximum variation in the normalised resistance is 0.24717; when the gap exceeds 2 mm, the curves corresponding to different temperatures essentially stabilise, and the resistance values no longer exhibit significant fluctuations. It can also be observed from Figure 8(b) that the equivalent resistance of the coil is approximately linearly positively correlated with temperature, with the resistance value continuing to increase as the temperature rises.

The calculation results indicate that the primary cause of significant deviations in the sensor's output voltage is the increase in the sensor's equivalent resistance as the temperature rises, which in turn alters the voltage division ratio in the measurement circuit. As changes in resistance inevitably lead to changes in the sensor coil's impedance, this results in variations in the sensor's output voltage, thereby affecting the gap measurement results. Compared to the gap, the influence of temperature on the sensor's equivalent inductance is negligible. Based on this characteristic, gap detection can be achieved by calculating the coil inductance, thereby suppressing measurement errors introduced by temperature.

3.2 Experimental research

3.2.1 Introduction to the test system

To verify the validity of the simulation results, a hollow planar coil, as shown in Figure 9, was fabricated from platinum wire with 20 turns. The sensor was subsequently encapsulated using ceramic and stainless steel materials; the physical structure is shown in Figure 10. Concurrently, a high-temperature test platform, as shown in Figure 11, was constructed. The complete experimental system primarily comprises a custom-made eddy current sensor, a heating furnace, an extensometer and an LCR analyser. The extensometer consists of a support base and a precision

displacement adjustment handwheel; during the experiment, all sensor parameters were acquired with high precision using the LCR analyser.

Subsequently, the sensor's temperature characteristic test was conducted using the voltage divider test circuit shown in Figure 13 (see Figure 5 for the circuit principle), revealing the variation in sensor output voltage with respect to the air gap at different ambient temperatures; the results are shown in Figure 14. The experimental data indicate that, under conditions where the measured gap remains constant, changes in ambient temperature cause significant deviations in the sensor's output voltage; furthermore, the higher the operating temperature, the greater the difference between the output voltage and the reference voltage calibrated at room temperature. This experimental phenomenon fully validates the aforementioned simulation conclusions, demonstrating that eddy current sensors calibrated at room temperature cannot be directly applied to high-temperature measurement scenarios.

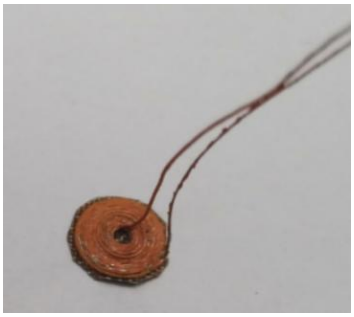


Figure 9 -Eddy current sensor coil



Figure 10 -Eddy current sensor



Figure 11 -High-temperature test bench



Figure 12 -LCR Inductance Analyser

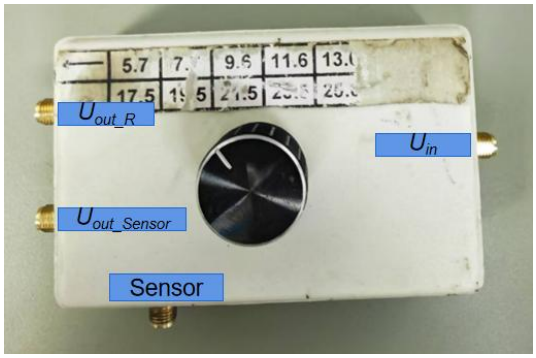


Figure 13 -Voltage divider circuit connector

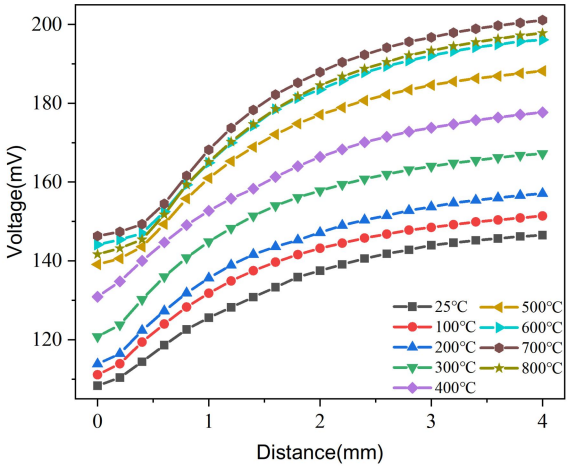
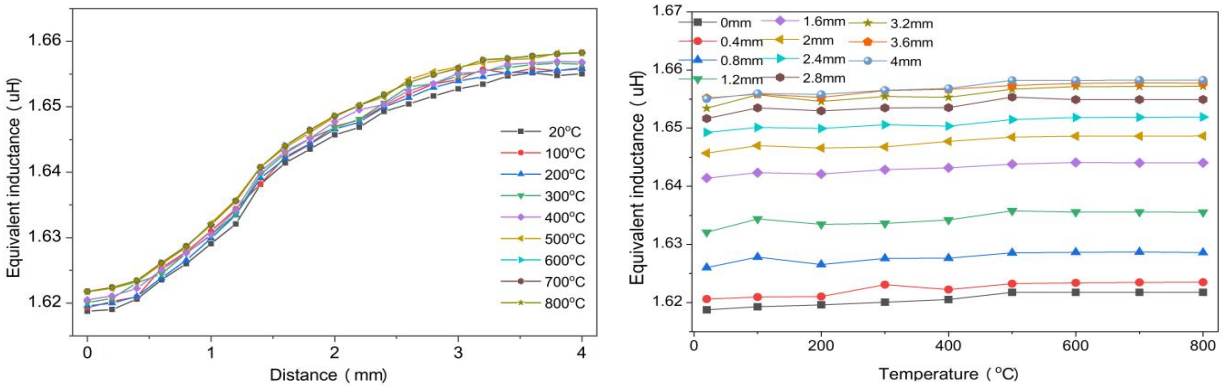


Figure 14 -Voltage across the sensor

3.2.2 *Experimental contents*

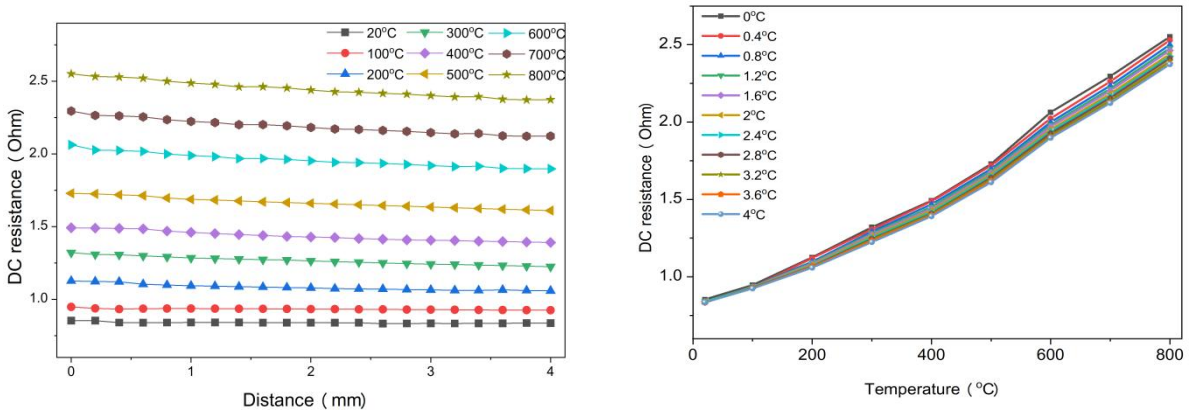
In the experiment, an LCR inductance analyser was used to measure the equivalent inductance, AC resistance and DC resistance of the sensor at different temperatures and with different air gaps; the data were plotted as shown in Figures 15 to 17:



(a)Variation in the equivalent inductance of an eddy current sensor with displacement at different temperatures

(b)Temperature-dependent variation in the equivalent inductance of an eddy current sensor at different air gaps

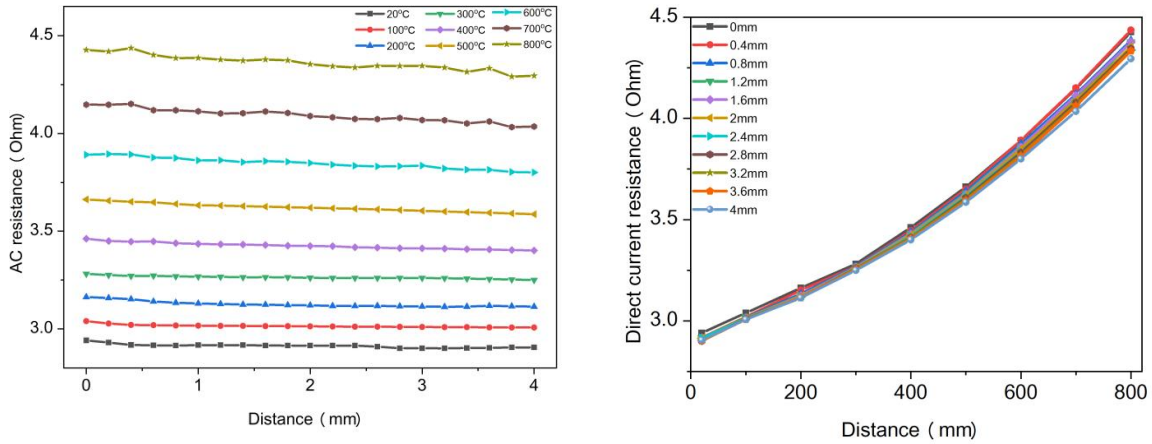
Figure 15 -Variation curve of the equivalent inductance of an eddy current sensor



(a)Variation in the DC resistance of an eddy current sensor with displacement at different temperatures

(b)Temperature-dependent changes in the DC resistance of an eddy current sensor at different gaps

Figure 16 -Curve showing the variation in DC resistance of an eddy current sensor



(a)Variation in the AC resistance of an eddy current sensor with displacement at different temperatures

(b)Temperature-dependent AC resistance of eddy current sensors at different gaps

Figure 17 -Curve showing changes in the AC resistance of an eddy current sensor

The results in Figure 15(a) indicate that the coil inductance increases gradually as the measured gap widens, and that the sensitivity of the coil inductance first increases and then decreases as the gap widens. This pattern is generally consistent with the simulation results. However, there is a marked discrepancy with the simulation results in Figure 7(b): the experimental data in Figure 15(b) indicate that the equivalent inductance of the coil is significantly more susceptible to temperature variations; when the temperature rises from room temperature to 800 °C, the maximum relative change in inductance at a gap of 3.2 mm can reach 0.2280109% of the inductance value at room temperature under these operating conditions, which may have a certain impact on the accuracy of gap measurement. The primary reason for this discrepancy is that, in the numerical simulation, the target object was modelled as an ideal rigid body, without accounting for the thermal expansion of the target object in a high-temperature environment; whereas, during the actual experiment, the rise in temperature caused the target object to expand thermally, thereby interfering with the inductance parameters. Furthermore, as shown in Figure 15(a), the sensor exhibits good linear characteristics within the 0.5–2 mm gap measurement range.

The graphs in Figures 16 and 17, showing the trends in AC and DC resistance, demonstrate that resistance varies in direct proportion to temperature; this corresponds with the simulation results. However, unlike the simulation results: as the temperature rises, the DC resistance is increasingly affected by the gap; at a temperature of 800°C, the DC resistance is most significantly affected by the gap, with a change of 0.1777 Ω within the 0–4 mm measurement range, representing approximately 20.8% of the resistance value at room temperature; The AC resistance also exhibits its greatest variation at 800°C, reaching 0.1292 Ω, which represents 4.4% of the AC resistance value at room temperature. Furthermore, as shown in Figure 8(a), when the gap exceeds 2 mm, the DC and AC resistances of the coil show almost no further change. However, the experimental results indicate that, within the measurement range exceeding 2 mm, the DC and AC resistances of the coil still decrease gradually with changes in the gap. This demonstrates that the coil resistance is influenced not only by temperature but also by the gap, and that the higher the temperature, the greater the influence of the gap on the resistance.

Figures 16 and 17 show the characteristic curves of the coil's DC and AC resistance, respectively. The experimental results indicate that both the AC and DC resistance of the coil exhibit a significant positive linear correlation with temperature; this pattern is consistent with the simulation findings. There are also discrepancies between the simulation and experimental results: as the temperature rises, the degree of interference on the DC resistance caused by changes in the air gap gradually increases. Under high-temperature conditions of 800°C, the influence of the air gap on the DC resistance reaches its maximum; within the measurement range of 0–4 mm, the change in DC resistance is 0.1777 Ω, which is approximately 20.8% of the DC resistance value at room temperature; Similarly, the AC resistance exhibits its greatest variation with gap size at 800 °C, with a value of 0.1292 Ω, accounting for 4.4% of the AC resistance at room temperature. Furthermore, the simulation results in Figure 8(a) show that when the gap exceeds 2 mm, the AC and DC resistances of the coil essentially stabilise and no longer vary with the gap; however, the experimental results indicate that once the gap exceeds 2 mm, the AC and DC resistances of the coil continue to decrease as the gap increases. This phenomenon suggests that the resistance of the sensor coil is simultaneously influenced by the coupled effects of temperature and gap, and that the higher the temperature, the greater the sensitivity of the resistance parameters to changes in the gap.

A synthesis of the simulation and experimental results reveals distinct differences in the characteristics of how temperature and air gap affect the inductance and resistance parameters of the eddy current sensor: the coil inductance is more sensitive to changes in the air gap, whilst the coil resistance exhibits a more pronounced response to temperature variations.

4. Design of an eddy current sensor measurement circuit

4.1 Circuit Design

The data indicates that, as the temperature changes, the equivalent inductance of the eddy current

sensor coil remains essentially constant, whilst the equivalent resistance increases gradually with rising temperature; when the gap changes, the equivalent inductance increases gradually with temperature, whilst the equivalent resistance changes only slightly. Experimental results show that, during gap measurement, changes in the ambient temperature lead to variations in the sensor's impedance, ultimately causing significant errors in the gap measurement results and affecting measurement accuracy.

To reduce measurement errors in high-temperature environments, this paper has formulated the temperature compensation scheme shown in Figure 18 based on the observation that the equivalent inductance of eddy current sensors is insensitive to temperature but sensitive to air gap changes. Furthermore, an eddy current sensor signal processing circuit, as shown in Figure 19, has been designed. This circuit utilises a high-speed inductance-to-digital conversion chip to digitise changes in inductance with high precision, enabling real-time analysis of the eddy current sensor's inductance. It is also equipped with an STM32 microcontroller for signal acquisition.

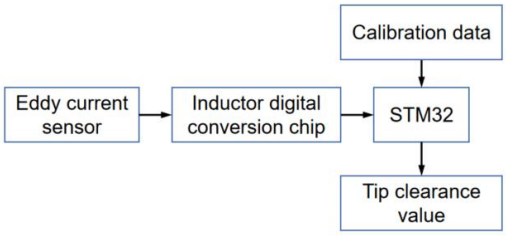


Figure 18 -Schematic diagram of the measurement circuit

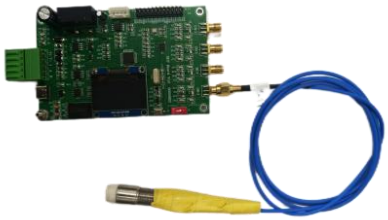


Figure 19 -Schematic diagram of the measurement circuit

4.2 Performance testing

Figures 20 and 21 show the measured gaps and the corresponding measurement errors at different temperatures and actual gaps, respectively. Analysis of the experimental data reveals that, as the distance between the sensor and the target increases, the measurement error generally follows a trend of first increasing and then decreasing; this pattern is determined by the inherent measurement characteristics of the eddy current sensor. As shown in Figure 20, across the entire measurement range of 0~4 mm, the maximum measurement error caused by temperature fluctuations does not exceed 200 μm; within the commonly used measurement range of 0.2~2.4 mm, the temperature-induced measurement error can be controlled to within 50 μm. The above results indicate that the eddy current sensor equipped with this measurement circuit offers good measurement accuracy, is capable of meeting the practical measurement requirements for tip clearance, and is suitable for tip clearance detection applications.

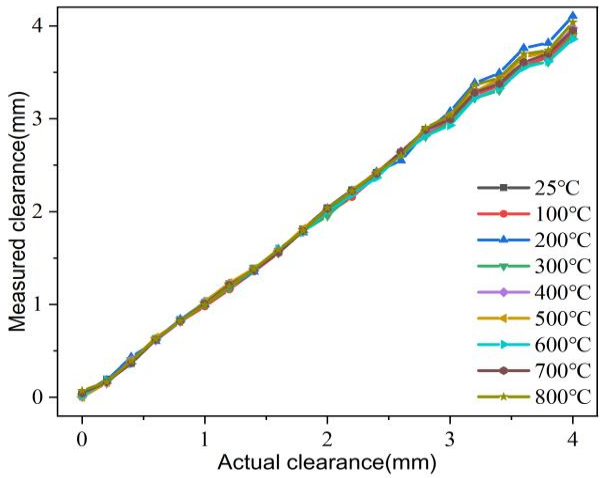


Figure 20 -Actual gaps at different temperatures and the corresponding measured gaps

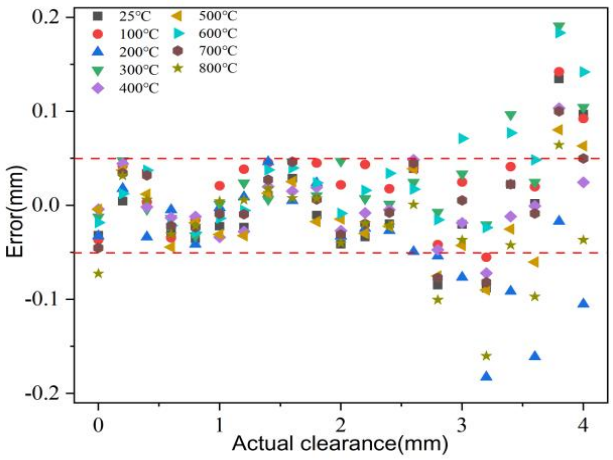


Figure 21 -Scatter plot of actual clearances at different temperatures and the corresponding measurement errors

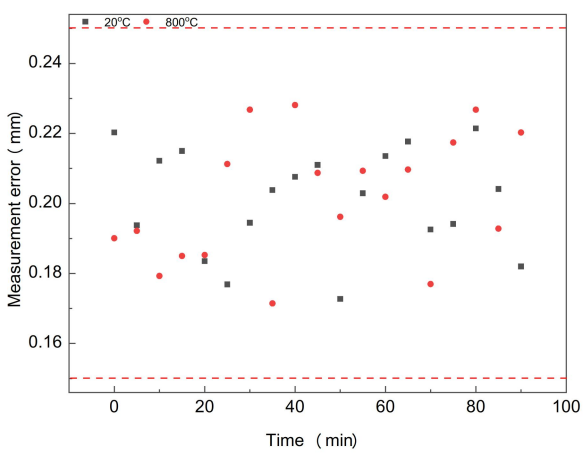


Figure 22 -Scatter plot showing the variation of measured values over time at an actual gap of 0.2 mm and temperatures of 20 °C and 800 °C

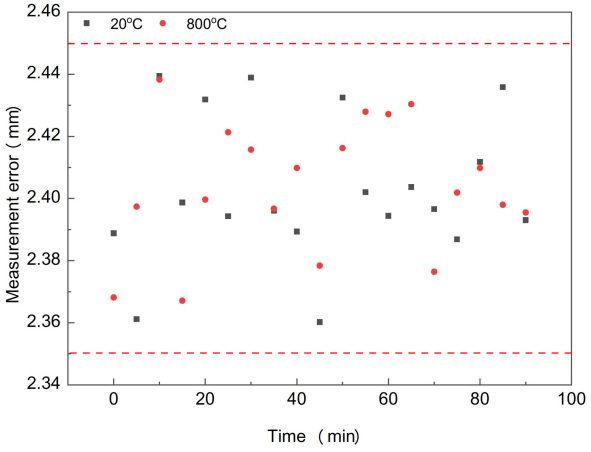


Figure 23 -Scatter plot showing the variation of measured values over time at an actual gap of 2.4 mm and temperatures of 20 °C and 800 °C

Figures 22 and 23 show the gap output values measured at room temperature and 800 °C for actual gaps of 0.2 mm and 2.4 mm, respectively. The experimental data indicate that in the stability test conducted at 800 °C with an actual gap of 2.4 mm, the maximum measurement error of the sensor was 39.8 μm after 45 minutes of testing. Furthermore, during the 90-minute test period, the error values for all operating conditions remained below 50 μm; consequently, the gap sensor designed in this paper demonstrates good temporal and temperature stability.

5. Conclusion

An analysis of the gap measurement results of eddy current sensors at different temperatures was conducted through both experimental and simulation methods. The study found that although eddy current sensors made with platinum wire coils exhibit high temperature resistance, they also suffer from significant temperature drift:

（1） When the temperature rises from room temperature to 800°C, the maximum change in equivalent inductance is only 0.2280109% of the equivalent inductance value at room temperature, whereas the change in DC resistance reaches 20.8% of the resistance value at room temperature. This indicates that when the ambient temperature changes, variations in the sensor's impedance (primarily its equivalent resistance) lead to significant errors in the measured gap values, thereby compromising measurement accuracy. Consequently, eddy current sensors calibrated at room temperature are unsuitable for gap measurement in high-temperature environments.

（2） Experimental and simulation results demonstrate that the equivalent inductance of eddy current gap sensors is significantly affected by the gap, whilst the equivalent resistance is more strongly influenced by temperature. Based on this finding, this paper has designed a measurement circuit based on the analytical variation of sensor inductance.

（3）Experiments have demonstrated that the eddy current sensor designed in this paper, based on analytical inductance, exhibits good measurement accuracy and stability when measuring tip clearance. Specifically, within the 0~4 mm measurement range, the error in sensor readings caused by temperature changes does not exceed 200 μm, and within the 0.2~2.4 mm measurement range, the measurement error does not exceed 50 μm.

6. Contact Author Email Address

The contact author phone number: +86 135 7210 7833. The email address: yglu@nwpu.edu.cn

7. Copyright Statement

The authors confirm that we and our organization hold copyright on all of the original material included in this paper and that we have obtained permission, from the copyright holder of any third

party material included in this paper, to publish it as part of our paper. The authors confirm that we give permission for the publication and distribution of this paper as part of the ICAS proceedings or as individual off-prints from the proceedings.

References

[1] Booth, T.C.; Dodge, P.R.; Hepworth, H.K. Rotor-tip Leakage: Part I—Basic Methodology. J. Engine Power 1982, 104, 154–161

[2] Liu Y,Tan L,Wang B.A review of tip clearance in propeller, pump and turbine [J]. Energies, 2018,11(9):2220.

[3] Mohamed, M.H.; Shaaban, S. Optimization of blade pitch angle of an axial turbine used for wave energy conversion. Energy 2013, 56, 229–239.

[4] Fujita H,Takata H. A study of configurations of casing treatment for axial flow compressors [J]. Bulletin of JSME,1984,27:1675—1681.

[5] Carney K S,Pereira J M,Revilock D M,et al. Jet engine fan blade containment usingan alternate geometry[J]. International Journal of Impact Engineering, 2009, 36(5) :720—728.

[6] Chen Wei, Du Farong, Li Yunqing. Fault Condition Identification in Aircraft Engine Rotor Scuffing [J]. Journal of Aerodynamics，2009,24(8):1706—1713.（in Chinese）

[7] Smith L H.Casing boundary layers in multi stage axial-flow compressor [M]. Amsterdam , Netherlands :Elesevier Publishing,1970:24-26.

[8] Hao, J. The investigation about civil aviation engine surge problem: The final solution for PW4000-94′ engine group 3 surge. In Proceedings of the 15th Aeroengine Design, Manufacturing and Application Technology Symposium, Beijing, China, 25–27 May 2013.

[9] Graf, M.B.; Wong, T.S.; Greitzer, E.M.; Marble, F.E.; Tan, C.S.; Shin, H.W.; Wisler, D.C. Effects of non-axisymmetric tip clearance on axial compressor performance and stability. J. Turbomach. 1998, 120, 648–661.

[10] García, I.; Beloki, J.; Zubia, J.; Aldabaldetreku, G.; Illarramendi, M.A.; Jiménez, F. An optical fiber bundle sensor for tip clearance and tip timing measurements in a turbine rig. Sensors 2013, 13, 7385–7398.

[11] Durana, G.; Amorebieta, J.; Fernandez, R.; Beloki, J.; Arrospide, E.; Garcia, I.; Zubia, J. Design, fabrication and testing of a high-sensitive fiber sensor for tip clearance measurements. Sensors 2018, 18, 2610.

[12] Lavagnoli, S.; Paniagua, G.; Tulkens, M.; Steiner, A. High-fidelity rotor gap measurements in a short-duration turbine rig. Mech.Syst. Signal Process. 2012, 27, 590–603.

[13] Violetti, M.; Skrivervik, A.K.; Xu, Q.; Hafner, M. New microwave sensing system for blade tip clearance measurement in gas turbines. In Proceedings of the 11th IEEE Sensors Conference, Taipei, China, 28–31 October 2012.

[14] Haase, W.C.; Haase, Z.S. Advances in through-the-case eddy current sensors. In Proceedings of the 2013 IEEE Aerospace Conference, Big Sky, MT, USA, 2–9 March 2013. Sensors 2024, 24, 5938 17 of 17

[15] Tomassini, R.; Rossi, G.; Brouckaert, J.F. Blade tip clearance and blade vibration measurements using a magneto resistive sensor.In Proceedings of the 11th European Conference on Turbomachinery Fluid dynamics & Thermodynamics, Madrid, Spain, 23–27 March 2015.

[16] Tomassini, R. Blade Tip Timing and Blade Tip Clearance Measurement System Based on

Magnetoresistive Sensors; Università degli Studi di Padova: Padova, Italy, 2016.

[17] Liu, Z.; Zhao, Z.; Lyu, Y.; Zhao, L. Experimental Investigation of Inductive Sensor Characteristic for Blade Tip Clearance Measurement at High Temperature. Sensors 2019, 19, 3694.

[18] Yepifanov S V，Li Q. Analysis of the error in the gas temperature and the thermocouple time constant measuring through gas turbine engine tests ［C］. Advances in Intelligent Systems and Computing，2020：325-336.